# Disruption of Large-Scale Brain Systems in Advanced Aging

**Jessica R. Andrews-Hanna**[1,2], **Abraham Z. Snyder**[3,4], **Justin L. Vincent**[1,2], **Cindy Lustig**[5], **Denise Head**[3,6], **Marcus E. Raichle**[3,4], and **Randy L. Buckner**[1,2,7,8,*]

[1]Department of Psychology, Center for Brain Science, Harvard University, Cambridge, MA 02138, USA

[2]Athinoula A. Martinos Center for Biomedical Imaging, Massachusetts General Hospital, Charlestown, MA 02129, USA

[3]Department of Radiology, Washington University School of Medicine, St. Louis, MO 63110, USA

[4]Department of Neurology, Washington University School of Medicine, St. Louis, MO 63110, USA

[5]Department of Psychology, University of Michigan, Ann Arbor, MI 48109-1043, USA

[6]Department of Psychology, Washington University in St. Louis, St. Louis, MO 63130-4899

[7]Department of Radiology, Harvard Medical School, Boston, MA 02155, USA

[8]Howard Hughes Medical Institute, Chevy Chase, MD 20815-6789

## SUMMARY

Cognitive decline is commonly observed in advanced aging even in the absence of disease. Here we explore the possibility that normal aging is accompanied by disruptive alterations in the coordination of large-scale brain systems that support high-level cognition. In 93 adults aged 18 to 93, we demonstrate that aging is characterized by marked reductions in normally present functional correlations within two higher-order brain systems. Anterior to posterior components within the default network were most severely disrupted with age. Furthermore, correlation reductions were severe in older adults free from Alzheimer's disease (AD) pathology as determined by amyloid imaging, suggesting that functional disruptions were not the result of AD. Instead, reduced correlations were associated with disruptions in white matter integrity and poor cognitive performance across a range of domains. These results suggest that cognitive decline in normal aging arises from functional disruption in the coordination of large-scale brain systems that support cognition.

## INTRODUCTION

Advanced aging is accompanied by cognitive decline even in the absence of disease. Several theories posit that cognitive deficits in normal aging arise from alterations in functional properties of coordinated brain systems or from subtle anatomical disconnection between brain regions that ordinarily function together, possibly due to white matter loss or demyelination (O'Sullivan et al., 2001; Pfefferbaum et al., 2000, 2005; Head et al., 2004; Salat et al., 2005). Based on the structural observation of age-associated white matter degeneration, O'Sullivan

et al. (2001) proposed the "disconnection" hypothesis: decline in normal aging emerges from changes in functional integration between systems of brain areas in addition to dysfunction of specific gray matter areas. However, the functional properties of large-scale brain systems and physiological interactions between brain areas have been difficult to measure.

Functional correlation methods based on analysis of spontaneous fluctuations within brain systems provide a powerful means of examining system integrity (Biswal et al., 1995; Greicius et al., 2003). The basis of these techniques is that functional MRI (fMRI) detects the spontaneous, low-frequency fluctuations that are coherent within large-scale systems, such as motor (Biswal et al., 1995) and sensory (De Luca et al., 2005) systems. Systems that participate in attention (Fox et al., 2006) and memory (Greicius et al., 2003; Vincent et al., 2006) have been similarly characterized.

Here we used these techniques to measure the integrity of a large-scale system that involves frontal and posterior brain regions (Shulman et al., 1997; Mazoyer et al., 2001). This system, often referred to as the "default network" (Raichle et al., 2001), is associated with internally directed mental states including remembering, planning, and related cognitive functions (Greicius et al., 2003; Vincent et al., 2006; Fransson, 2005; Buckner and Carroll, 2007).

Specifically, the current study examined the effects of aging on the functional integrity of the default network and considers both general age trends as well as individual differences in cognition. In the first part of the study, as a measure of functional integrity, we investigated whether regions that are normally temporally correlated in young adults (specifically, medial frontal, posterior cingulate/retrosplenial cortex [pC/rsp], and medial temporal regions) become less correlated with increasing age. To examine whether reduced functional integrity is associated with structural disruption, we next explored the relationship between functional correlations and white matter integrity as measured using diffusion tensor imaging (DTI). We hypothesized that older individuals with the most degraded white matter would exhibit the weakest functional correlations. In the last part of the study, we examined whether individual differences in functional correlation strength predicted individual differences in cognition. We reasoned that if large-scale disruption in brain systems were a source of age-associated cognitive decline, measurements of functional system integrity would correlate with composite measures of cognitive function. We also examined the integrity of the dorsal attention system (Corbetta and Shulman, 2002) to explore whether aging broadly affects multiple brain systems.

To foreshadow the results, older adults showed robust decreases in functional correlations in the default network. Disruption of the dorsal attention system was also observed. Reduced correlations associated with white matter degradation and poor cognitive performance, suggesting that age-associated disruption of large-scale brain systems is an important contributor to cognitive decline.

## RESULTS

### Correlations between Brain Regions Are Markedly Reduced in Advanced Aging

Initial analyses examined whether the strength of low-frequency functional correlations declined with age. Results revealed that correlation strengths were markedly reduced, in particular between those regions widely separated along the anterior-posterior axis. Exploratory analyses using whole-brain maps of correlation strength and direct comparisons between age groups confirmed this observation.

**A Priori Regional Analysis—**To ensure that regional measurements were made in an unbiased manner, all regions of interest (ROIs) used in the present analyses were defined in an independent data set consisting of equal numbers of young and old adults (described in more

detail in the Experimental Procedures section). Regions were defined in the medial prefrontal cortex (mPFC), the pC/rsp, the bilateral lateral parietal cortex (LatPar), the bilateral hippocampal formation (HF), and the bilateral parahippocampal cortex (PHC). Because the data were spatially smoothed, the anatomic boundaries of the regions may extend into voxels within adjacent structures (Vincent et al., 2006). Each region was subsequently carried forward as an a priori ROI for further analyses.

Regional analysis proceeded by calculating the correlation coefficient between a seed region and a second predefined target region. For each ROI, the mean time course was extracted and the correlation coefficient with the other ROI was computed using Pearson's product-moment correlation. The resulting correlation, $r$, reflects the strength of the functional relationship between the two regions. All statistical tests on correlation coefficients were performed on Fisher $r$-to-$z$ transformed correlation coefficients, $z(r)$, which are approximately normally distributed over the sample (Vincent et al., 2006). However, for simplicity of interpretation, we report the correlation coefficients.

We first examined whether functional correlations between anterior mPFC and posterior pC/rsp regions were compromised in aging. These two regions were selected for analysis because they represent two major components of the default network (Greicius et al., 2003; Shulman et al., 1997; Raichle et al., 2001; Fransson, 2005) and are presumed to interact through long-range white matter pathways. Results revealed a dramatic reduction in correlation between the two groups [young: $r = 0.43$, old: $r = 0.00$; independent samples t test: $p < 0.001$; Figure 1, plotted as $z(r)$]. The correlation strength was dependent on age within the older adult group such that the oldest individuals exhibited the smallest correlations (Figure 1: $r = -0.53$; $p < 0.001$). Thus, both the between-group comparison and the correlation with age among older adults converged to suggest that aging has a marked effect on low-frequency functional correlations between anterior and posterior cortical regions.

We next explored the degree to which these correlation reductions were present in nine older adults without amyloid beta (A$\beta$) deposition as determined by positron emission tomography (PET) using C-11 labeled Pittsburgh Compound B ([$^{11}$C]PIB) (PIB-PET). The mean anterior-posterior functional correlations for this subset of participants closely matched the correlation for the entire old group (old overall: $r = 0.00$, old PIB-negative: $r = 0.03$). Using only this subset of PIB-negative older adults, the age-related reduction in correlation strength between the anterior and posterior regions was significant (young: $r = 0.43$, old PIB-negative: $r = 0.03$; independent samples t test: $p < 0.001$). The presence of the effect in the PIB-negative older adults suggests that the age-dependent decline in anterior-posterior functional correlations occurs independently of AD.

To further explore the effects of aging on functional correlations, Figure 2 shows the topographical pattern of age-related reductions in correlation along the brain's anterior-posterior axis. For this analysis, a seed region was correlated with every voxel (point) along the anterior-posterior axis in both young and older adults, allowing visualization of the strength and 2D pattern of correlations across the brain. [This visualization strategy is similar to that used for DTI data in Pfefferbaum et al. (2005)]. Correlation with a seed region in the mPFC resulted in weaker correlations in posterior regions at or near the pC/rsp in the older group as compared with the young group (Figure 2A). Similarly, older adults exhibited weaker correlations in anterior regions for a seed region placed in the pC/rsp (Figure 2B).

We next investigated whether functional disruptions extended to additional regions within the default network by examining functional correlations between all combinations of a priori ROIs (Figure 3). The following comparisons revealed group correlation differences at a significance threshold that survived Bonferroni correction using a critical alpha of 0.005: mPFC versus

LatPar, pC/ rsp versus LatPar, LatPar versus HF, LatPar versus PHC, and PHC versus HF. In each of these comparisons, older adults exhibited reduced correlations. While two comparisons were not significant (mPFC versus HF comparison and the pC/rsp versus PHC comparison), both showed numerically weaker correlations in the older adults, suggesting that reductions in functional correlations were present across the entire brain system.

**Influence of Task on Functional Correlations**—Given that all participants were engaged in a semantic-decision task, an important question is whether systematic group differences in task-related activity influence the observed differences in functional correlations. To answer this question, we first estimated evoked responses within the mPFC and the pC/rsp by using a general linear model to model task minus fixation. We then extracted the most informative estimates of response magnitude by averaging three successive time points corresponding to peaks within the young and old group. Group differences in response magnitude were observed in the mPFC (young: percent signal change = −0.05, old: percent signal change = −0.01; independent samples t test: p = 0.05) and the pC/rsp (young: percent signal change = −0.04, old: percent signal change = 0.004; independent samples t test: p < 0.01), indicating that older adults exhibited weaker task-induced deactivations in these regions (see also Lustig et al., 2003). We also observed a significant relationship between the magnitude of evoked response within each region and our measure of functional correlation between the mPFC and the pC/rsp (mPFC: $r = −0.33$, p < 0.01; pC/rsp: $r = −0.37$, p < 0.001). In other words, participants who exhibited the strongest task-induced deactivations also exhibited the strongest functional correlations. Finally, within the old group alone, neither of the evoked responses significantly correlated with age (mPFC: $r = 0.16$, p = 0.24; pC/rsp: $r = 0.27$, p = 0.09).

To explore whether the effect of task-related activity on anterior-posterior functional correlations accounts for our observations, we included the evoked responses within the mPFC and the pC/rsp as simultaneous regressors in a multiple regression model with mPFC-pC/rsp functional correlation as the dependent variable. Performing an independent samples t test on the residuals yielded a significant group difference (p < 0.001), indicating that there are group changes in functional correlations that persist after effects of task have been removed. Similarly, when partialling out the effect of evoked responses on both age and anterior-posterior functional correlations within the old group alone, functional correlations remained strongly negatively correlated with age ($r = −0.48$; p < 0.001). Thus, the evoked responses did not account for the observed relations, although it is interesting to note that, by all measures, there are age-related disturbances in these key nodes of the default network.

In addition to controlling for group differences in task activation, we also controlled for group differences in performance accuracy on the semantic classification task (young: 95%, old: 89%; p < 0.001). After controlling for these differences, the group difference in functional correlations remained robust (p < 0.001), and the functional correlation × age relationship did as well ($r = −0.48$; p < 0.001).

**Influence of Variance Differences**—The time course variance of all a priori ROIs, except for the mPFC, differed between groups at a level that survived correction for multiple comparisons (Bonferroni correction: critical alpha = 0.01; Figure 3). Variances associated with the pC/rsp and the LatPar were significantly higher in the young adult group (independent samples t test for each region: p < 0.001), and the variances within the HF and the PHC were significantly higher in the older adult group (independent samples t test for each region: p < 0.001). Thus, the direction of the effect was not consistent by group. We suspect that the increased variance in the HF and PHC in aging is related to medial temporal atrophy and consequent volume averaging of cerebrospinal fluid. As a further control analysis, we examined the influence of signal variance on the anterior-posterior functional correlations. The group difference in functional correlations between the mPFC and pC/rsp remained significant

(independent samples t test: $p < 0.001$), suggesting that differences in regional variance did not account for the reduced age-associated functional correlations (see Supplemental Materials available online for additional control analyses).

**Whole-Brain Exploratory Analysis—**The above targeted regional analyses were complemented with whole-brain exploratory maps. Maps were created by computing, at each voxel within the brain, the correlation strength with seed regions placed in the mPFC and pC/rsp. The mPFC and pC/rsp maps were computed separately for each age group (young and old), and maps showing statistical differences between the two groups were prepared (Figure 4).

In young adults, a robust functional correlation map was obtained for the mPFC seed region including positive correlations in medial parietal cortex and LatPar extending into pC/rsp (Figure 4A). In older adults this pattern was topographically unchanged, but less robust. A direct comparison of the correlation maps between the two groups illustrated that these regional differences were significant: both medial parietal and lateral parietal regions were correlated with the mPFC to a significantly greater degree in the young adults. Conversely, for a seed placed in the pC/rsp, older adults exhibited reduced functional correlations along the frontal midline and LatPar, with some suggestion of reduced correlations within the medial temporal lobe (Figure 4B).

**Dorsal Attention System Analysis—**In order to examine the generality of reduced functional correlations in aging, we performed similar analyses between regions within the dorsal attention system. This system includes a set of brain regions commonly recruited during tasks requiring directed attention (Corbetta and Shulman, 2002) and has previously been explored in young adults using similar functional correlation methods (Fox et al., 2006). Significant group differences in functional correlations (at a level corrected for multiple comparisons using the Bonferroni procedure, $p < 0.005$) were present for the following combinations of seed and target ROI: intraparietal sulcus (IPS) versus middle temporal area ($MT^+$), ventral intraparietal sulcus (vIPS) versus inferior precentral sulcus (PrCeS), and vIPS versus $MT^+$ (Figure 5). The correlations between the IPS versus vIPS, the vIPS versus frontal eye fields (FEF), and the FEF versus PrCeS were significant at an uncorrected level of $p < 0.05$. There were no significant group differences in time course variance within any of the external attention ROIs.

**Visual Cortex ROI Control Analysis—**The first part of this study illustrated that long-range correlations between regions within two large-scale brain systems decline in advanced age. An immediate question is whether such reductions are present between *all* functionally correlated regions. As a control measure, we investigated the correlation strength between left and right visual regions in both groups, as early visual areas have been shown to robustly activate in response to visual stimuli in both young and old adults, although perhaps not to an equal extent (Buckner et al., 2000; but see Aizenstein et al., 2004). Moreover, posterior callosal fibers that mediate interhemispheric connections between visual regions (Myers, 1962) appear largely intact in normal aging, whereas anterior callosal fibers that mediate interhemispheric connections between sensorimotor regions (Matsunami and Hamada, 1984) do not (O'Sullivan et al., 2001; Pfefferbaum et al., 2005; Head et al., 2004; Salat et al., 2005). Recent evidence also suggests that the sensorimotor system may be disrupted in aging (Wu et al., 2007). For this reason, we decided to compare the correlation coefficient between left and right visual ROIs corresponding approximately to left and right V2. Literature in nonhuman primates shows that left area V2 is connected to corresponding points in the right hemisphere by long but direct connections that travel through the posterior corpus callosum (Myers, 1962). Thus, if functional correlations between all widely separated brain regions were disrupted in aging, one would expect that our analysis within the visual system would be similarly affected. Results

revealed similar group correlation coefficients (young: $r = 0.62$, old: $r = 0.60$; independent samples t test: $p = 0.45$) and a lack of association with age in the older adults (Figure 6A: old: $r = 0.17$, $p = 0.22$). The effect is illustrated topographically by plotting the correlation strengths (after $r$-to-$z$ transformation) along the x axis (Figure 6B).

## Reduced Correlations Associate with Decreased White Matter Integrity in Older Adults

The above results show decreased functional correlations across the default network and the dorsal attention system in advanced aging. Advanced aging is accompanied by compromised brain structure, including reduced integrity of white matter [for a review see Sullivan and Pfefferbaum (2006)]. Accordingly, we hypothesized that more severe white matter compromises would be associated with reduced functional correlations. Since the anterior-posterior correlations in the default network were most robustly affected by age, we chose this measure as our dependent variable in the following analyses. For each older subject, the mean anisotropy within a large white matter region was measured and correlated with the functional correlation strength between the mPFC and pC/rsp (Figure 7). Results revealed that reductions in functional correlations were associated with reduced diffusion tensor anisotropy measured by DTI (Figure 7A: $r = 0.39$, $p < 0.01$). This relationship persisted in the older adult group after controlling for the effect of age on both variables (Figure 7B: partial $r = 0.33$, $p < 0.05$), suggesting that the effect accounted for variance between individuals beyond that accounted for by age alone.

## Reduced Correlations Associate with Cognitive Deficits in Older Adults

To explore the cognitive significance of the observed functional disruptions, we examined whether alterations in functional correlations relate to cognitive abilities in the older individuals. Forty older participants completed psychometric tests measuring a variety of cognitive processes. We collapsed these measures into three composite indices of function (executive function, memory, and processing speed) by combining the scores from individual tests that each measured similar cognitive abilities. The correlation strength between the mPFC and the pC/rsp significantly associated with the memory composite before controlling for the effect of age (Figure 8A; executive: $r = 0.26$, $p = 0.11$; memory: $r = 0.48$, $p < 0.01$; speed: $r = 0.24$, $p = 0.14$). When controlling for the effect of age on both variables, the relationship between correlation strength and cognition was present for all three domains (Figure 8B; executive: partial $r = 0.41$, $p < 0.01$; memory: partial $r = 0.40$, $p < 0.01$; speed: partial $r = 0.35$, $p < 0.05$). Those individuals exhibiting the lowest functional correlations also exhibited the poorest cognitive test scores. It is important to note, however, that age-related disruptions in the brain that interact with the default network, such as neurotransmitter depletion, may also contribute to cognitive variability (Bäckman et al., 2000). Our results, which demonstrate a strong relationship, are based on correlational analyses and therefore will require further exploration to understand fully.

## DISCUSSION

The idea that advanced aging may be associated with disruption of the coordinated activity of brain systems has arisen based on the observation of structural alterations in white matter integrity (O'Sullivan et al., 2001; Sullivan and Pfefferbaum, 2006) and nonspecific functional activity patterns (Park et al., 2004; Gazzaley et al., 2005; Cabeza, 2002). Until recently, the functional properties of large-scale brain systems and interactions between brain areas in individuals have been difficult to measure. Using a particular measure of functional integrity, we show that the coordinated activities of large-scale brain systems are robustly affected by aging, especially those between anterior and posterior components of the default network. Using PIB-PET amyloid imaging, we further demonstrate that the correlation reductions appear to be independent of preclinical AD pathology. Moreover, these differences are associated with

disrupted cognitive performance across a range of domains, including executive function. Measurement of white matter integrity using DTI revealed a clear association between disruption of the anterior-posterior functional correlations and mean regional anisotropy. We expand on the implications of these findings below and the caveats associated with the methods.

## Measuring Disruption of Large-Scale Brain Systems in Older Adults using fMRI

The present analyses explored functional integrity in a large sample of young and old adults by measuring fMRI signal correlations between regions within large-scale brain systems. Extracting estimates of activity correlations is a powerful means of measuring disruption of brain systems in advanced aging. Using estimates of effective connectivity, Grady et al. (2003) have recently observed that functional correlations between groups of older and younger adults differ in ways that relate to cognition. Here we found that the anterior-posterior functional integrity of the default network, measured using correlation coefficients, dropped from 0.43 to 0.00 in older adults. Before discussing the implications of these results, it is worth noting some of the strengths and weaknesses of our approach.

Low-frequency activity correlations are present and detectable in many brain systems by using fMRI. Originally described by Biswal et al. (1995) in the sensorimotor system, spontaneous correlations have since been observed in young adults within brain systems important to memory (Greicius et al., 2003; Vincent et al., 2006) and attention (Fox et al., 2006). While the origins of the activity events driving spontaneous correlations remain poorly understood, they are present during anesthesia and have been shown to track direct and indirect anatomic connectivity between regions (Vincent et al., 2007).

Several methodological concerns need to be addressed before the present observations can be interpreted. Older adults differ from young adults in brain anatomy and brain motion during imaging, both of which cause differences in variance properties that influence measured functional correlations between brain regions. A number of control analyses were performed to address concerns that our observed effects were simply due to systematic differences in the fMRI signal (Buckner et al., 2000; D'Esposito et al., 2003). First, the effects persisted after controlling for variance, and similar results were obtained when controlling for motion. Second, the effects also persisted in variance-matched subsets of participants (see Supplementary Materials). Finally, correlations between right and left visual brain regions that were predicted to be minimally affected in aging were largely conserved in our analyses. Thus, while measurement differences including variance in the fMRI signal differ between age groups, such differences almost certainly do not account for the present results. Moreover, the observation that reduced blood oxygen-level dependent (BOLD) correlations were associated with both DTI evidence of white matter differences and impaired cognitive performance reinforces the impression that the brain normally loses functional integrity in the course of advanced aging.

## Implications of Functional Disruption of Large-Scale Brain Systems in Normal Aging

Accumulating evidence suggests that aging is associated with multiple cascades that arise from separate patho-physiological processes, each associated with distinct cognitive sequelae (Hedden and Gabrieli, 2004; Buckner, 2004). Specifically, a two-factor model of aging is commonly advocated that proposes a separation between memory disruption linked to AD and executive dysfunction associated with compromised frontal-striatal systems. While the pathology of AD has been extensively explored, less is known about how functional disruption arises in normal aging. Furthermore, information concerning which brain systems are functionally disrupted in aging is lacking, although the consensus derived from structural analyses is that anterior brain regions show preferential gray matter volume loss and reduced white matter integrity (Sullivan and Pfefferbaum, 2006; Raz, 2000). The present study

identifies a form of age-associated disruption that affects large-scale brain systems, is linked to white matter integrity, broadly impairs cognition, and is observed in older adults lacking the Aβ pathology associated with AD.

One possibility is that we are observing at a functional level the consequences of decreased white matter integrity, although it must be noted that the data connecting the anatomical and functional observations are presently based only on a cross-sectional association. In addition to decreased white matter integrity, other age-related changes such as gray matter atrophy, neurotransmitter depletion, or both may contribute to the group differences in functional correlations. Nevertheless, our observations suggest that within the context of globally intact brain systems, subtle changes accumulate over time in advanced aging that disrupt the coordination of large-scale brain systems. Although BOLD signal correlation reductions were widespread throughout the default network and the dorsal attention system, they were not present in all brain systems as shown by our control analysis of visual cortex. These patterns are qualitatively consistent with the widespread white matter changes in aging that may preferentially affect anterior brain regions (O'Sullivan et al., 2001; Pfefferbaum et al., 2000, 2005; Head et al., 2004; Salat et al., 2005). In addition, the functional correlation reductions were associated with cognitive decline across multiple domains, prominently including executive function and general slowing, although one cannot rule out added effects on cognitive variability from brain regions that may interact with the default network.

It is important to note that disruption of large-scale brain systems measured using low-frequency fMRI correlations is not restricted to normal aging. Greicius et al. (2004) observed that individuals with AD show reduced correlations in the default system, especially pertaining to the medial parietal and medial temporal regions. Our present results, in particular the analysis of individuals without amyloid deposition, show that normal aging is associated with a form of system disruption that is distinct from that associated with AD. Schizophrenia (Liang et al., 2006), depression (Anand et al., 2005), ADHD (Tian et al., 2006), autism (Cherkassky et al., 2006), and spatial neglect (He et al., 2007) have also been associated with reduced functional correlations, suggesting that multiple disorders may be linked to functional disruption of large-scale brain systems. In the seminal work of Norman Geschwind, multiple disconnection syndromes resulted from lesions to distinct brain systems or components of brain systems (Geschwind, 1965). Echoing his early work, our findings, when taken in the context of the existing literature, may reveal a common consequence of a family of disorders that reflect more subtle forms of disconnection. While many of these disorders may be associated with loss of functional correlations within large-scale brain systems, each may manifest in distinct ways, depending on the specific brain systems involved. With regard to aging, we have shown that functional correlations within the default network and the dorsal attention system are severely disrupted, whereas functional correlations within the visual system are affected only minimally. Thus, first-order analyses suggest that aging may be associated with widespread disruptions in higher-order brain systems and may preferentially spare lower-order sensory systems.

A novel direction for future work will be to explore, in large samples that span multiple disorders, whether the functional disruptions that distinguish different disorders can be characterized. Within the spectrum of normal aging and AD, we suspect that the aging effects observed here, which were most robust between anterior and posterior brain regions, will be found to be distinct from additive influences of early-stage AD that preferentially target posterior systems linked to the medial temporal lobe. Another open question concerns whether there is a link between the commonly observed age-associated increases in task-related activity (Cabeza, 2002; Reuter-Lorenz, 2002) and the present reductions in functional correlations among brain regions. An intriguing possibility is that disrupted coordination of large-scale brain systems leads to inefficient processing that is compensated for by increased recruitment of available neural resources.

# EXPERIMENTAL PROCEDURES

## Participants

Study participants included 38 young adults and 55 older adults recruited from the students and community of Washington University in St. Louis and the local Alzheimer's Disease Research Center (ADRC). These participants represented a superset of individuals whose data was previously analyzed using traditional fMRI methods (Lustig and Buckner, 2004). These participants are distinct from those made publicly available in Buckner et al. (2000) and analyzed by Greicius et al. (2004). Demographic information for included participants is listed in Table 1. Individuals with excessive movement during fMRI (n = 4) or poor signal-to-noise (n = 3) were excluded. Additional individuals were excluded because the magnitudes of the variance of their fMRI time courses were greater than 3 standard deviations (SD) from the group mean (n = 4), as was a single older adult whose estimated network correlation strength was more than 3 SD from the mean. Procedures were completed in accordance with the Washington University Human Studies Committee guidelines.

## Image Acquisition

All images were acquired using a 1.5T Siemens Vision Scanner (Erlangen, Germany). Details regarding head stabilization, vision, and communication tools are described in Lustig and Buckner (2004) and only briefly described here. A high-resolution structural T1-weighted MPRAGE image was collected for each participant ($1 \times 1 \times 1.25$ mm, TR = 9.7 s, TE = 4 s, flip angle = 10°, TI = 20 ms, TD = 200 ms) followed by rapid event-related functional imaging using an asymmetric spin-echo sequence sensitive to BOLD contrast (TR = 2.5 s, T2* evolution time = 50 ms, 180 offset = −25 ms). Two relevant functional runs were collected (each run: 116 whole-brain acquisitions, $3.75 \times 3.75$ mm in-plane resolution, 16 slices 8 mm thick, aligned to the anterior-posterior commissure plane).

During the two BOLD runs used in this study, participants were engaged in a semantic classification task. Specific task details are outlined in Lustig and Buckner (2004). Each run began with 10 s of passive fixation, followed by 116 trials, each lasting 2500 ms. Two-thirds of trials included a semantic classification task where subjects made a button response to classify visually presented words as living or non-living objects. One-third of trials were passive fixation trials. Each 2500 ms trial was composed of 2000 ms of task or fixation followed by a 500 ms intertrial interval consisting of a fixation crosshair. Trials were randomly intermixed and counterbalanced across participants.

## Data Preprocessing

Functional data were first preprocessed to reduce image artifacts and remove timing differences between slices that resulted from asynchronous slice acquisition. Odd/even slice intensity differences resulting from acquisition of interleaved slices were eliminated, and head movement within and across runs was removed using rigid body translation and rotation. Anatomical and functional data were transformed to atlas space (Talairach and Tournoux, 1988; Maccotta et al., 2001) using an atlas target composed of a merged young-adult and older-adult reference (Buckner et al., 2004), and data were resampled to 2 mm isotropic voxels. Finally, drift was corrected by removing the linear slope on a voxel-by-voxel basis, and whole-brain signal intensity was normalized to a mean of 1000 for each functional run.

## Functional Correlation Analysis between Regions

Several additional steps, described in previous studies (Vincent et al., 2006; Fox et al., 2005), were taken to prepare the data for correlation analysis. First, low- and high-frequency components of the atlas-aligned BOLD data were removed using a temporal band-pass filter

retaining 0.009 Hz< f< 0.08Hz. Next, data were spatially smoothed using a Gaussian kernel of 6 mm full-width at half-maximum. Removal of several spurious or nonspecific sources of variance was accomplished by regression of the following variables: (1) the six movement parameters computed by rigid body translation and rotation in preprocessing, (2) the mean whole-brain signal, (3) the mean signal within the lateral ventricles, and (4) the mean signal within a deep white matter ROI. The first temporal derivative of each time course was also included in the regression procedure to account for temporally shifted nuisance waveforms. Regression of each of these signals was computed simultaneously and the residual time course was retained for the following correlation analysis.

Two forms of analysis were performed to yield (1) correlation strengths between pairs of regions and (2) correlation maps between a seed region and all voxels across the whole brain. For analysis using a priori regions, the time course was extracted from each region and the correlation coefficient was computed using Pearson's product-moment formula. Whole-brain exploratory analysis similarly involved computing the correlation coefficient between the averaged time course at the seed region and the time course for each voxel across the whole brain. The resulting correlation maps were converted to $z$ values using Fisher's $r$-to-$z$ transformation (Zar, 1996). We also evaluated voxel-wise correlation strengths on lines connecting two regions along the anterior-posterior axis. Such plots are particularly informative for visualizing the correlation profile across a specific anatomical cross-section of the data. Significance testing of between-group effects was performed using random-effects analyses.

## ROI Definition

To create regions in an independent and unbiased manner, an initiating pC/rsp seed was selected from a conjunction analysis of several functional studies (Buckner et al., 2005) and applied to a separate dataset (Buckner et al., 2000) of eight young (21.3 years; four male) and eight old (77.4 years; four male) adults. While this initiating seed was somewhat arbitrary, similar results are obtained using almost any of the regions that are commonly part of the default network (e.g., Shulman et al., 1997; Mazoyer et al., 2001). The Buckner et al. (2000) dataset was then examined for correlations with the pC/rsp seed. Based on the pattern of the correlations, we extracted peak coordinates corresponding to the mPFC, the HF, and the PHC. Regions were defined around these peaks as all contiguous voxels exceeding a $z$-transformed correlation coefficient of 0.1 within a radius of 4–8 mm. The peak coordinates corresponding to the LatPar and a newly defined pC/rsp ROI were selected in a similar manner using the correlation map for a seed in the HF, obtained in the above analysis. We have demonstrated in a previous study that the correlational pattern of both left and right HF is highly similar (Vincent et al., 2006). Thus, in order to increase power in the present analyses, we used bilateral, as opposed to unilateral, ROIs. Using this procedure, the following a priori ROIs were created (coordinates are in the atlas space of Talairach and Tournoux, 1988): mPFC (1, 40, 16), pC/rsp (−1, −50, 26), LatPar (L: −45, −67, 26; R: 53, −65, 26), HF (L: −23, −25, −12 ; R: 23, −25, −12), and PHC (L: −25, −39, −10; R: 25, −39, −10).

External attention system ROIs were defined using identical methods to the ones described above. Specifically, peak coordinates in selected regions of the cortex were identified on the group-averaged Fischer's $r$-to-$z$ transformed correlation map for an 8 mm (radius) spherical seed in the IPS, a region selected from a previous functional correlation study (Fox et al., 2006). Regions were defined around peak coordinates in or near the vIPS and FEF, and in and around the superior precentral sulcus, the PrCeS, and the MT[+]. Similarly, the peak coordinates corresponding to the IPS were selected using the correlation map for a seed in the vIPS, obtained from the above analysis.

Using this procedure, the following a priori ROIs were created for further analysis of the dorsal attention system: IPS (L: −21, −71, 44; R: 23, −63, 50), vIPS (L: −27, −75, 24; R: 31, −79, 22), FEF (L: −27, −7, 50; R: 27, −1, 54), PrCeS (L: −45, −1, 34 ; R: 45, 5, 34), and MT$^+$ (L: −47, −75, −4; R: 49, −69, 4).

Using an initiating visual seed from a separate study (Konishi et al., 2000), two control ROIs were also created: one centered in the left visual cortex (−19, −95, 2) and another centered in the right visual cortex (19, −95, 2). All of the ROIs were then carried forward as a priori seed and target regions for further analysis in the present dataset.

## DTI

A subset of 44 older adults (76.2 years; range = 60 to 93; 13 male) were imaged in an additional data session that included DTI. The DTI acquisition protocol was identical to Head et al. (2004), using a spin-echo echo-planar imaging sequence ($1 \times 1 \times 1.25$ mm, TR = 7.2 s, TE = 108 ms, 36 slices at 4 mm at 2.5 mm$^2$ in-plane resolution, interpolated to 1.25 mm$^2$). Four acquisitions were acquired for each participant and averaged. Diffusion-weighted data were coregistered to the structural data, and the diffusion tensor at each voxel was computed using standard least-squares techniques, with the derived measure of mean diffusion anisotropy used for this analysis being $A_\sigma$, ranging from 0 to 1 (Conturo et al., 1996; see Head et al., 2004 for implementation as used here). Diffusion anisotropy represents the degree to which water molecules diffuse along a particular axis, with values closer to the upper limit of 1 indicating strong directionality (typical of healthy myelinated white matter) and values closer to 0 indicating isotropic diffusion (indicating degraded white matter).

For each participant, the mean diffusion anisotropy was calculated for a large ROI (Figure 7A; Figure S2) that was manually traced using Analyze-AVW Software (Mayo Medical Foundation, Rochester, MN) on a mean anisotropy map from an independent sample of 44 older adults (76.6 years; range = 60 to 91; 14 male) otherwise not analyzed in the present study. Specifically, the ROI was traced on the mean diffusion weighted anisotropy image as opposed to the T1-weighted structural image in order to minimize the inclusion of gray matter and because of distortion of the DTI volumes. The ROI was demarcated to include white matter within the medial part of the centrum semiovale for each hemisphere on all slices from z = 21 to slice z = 41. The rostral and caudal y coordinates for the ROI in each hemisphere were y = 34 and y = −65, while the x coordinates in the left hemisphere ranged from x = −29 to x = −14, and in the right hemisphere, from x = 15 to x = 28. The bilateral ROI included several white matter bundles such as the corona radiata, superior longitudinal fasciculus, and cingulum bundle. These regions have been shown to exhibit age-associated white matter disruption (Pfefferbaum et al., 2000, 2005; Head et al., 2004), and our selection of this relatively large region allows for a stable estimate of white matter disruption in individual participants. White matter disruption in aging is diffuse with an anterior-to-posterior gradient. Our region captures the overall health of white matter within a participant, but it is not meant as a selective measure of specific fiber bundle integrity. Mean anisotropy values within this ROI were calculated for each available participant in the present data set and were entered into regression analyses that compared the DTI measures to the strength of functional correlations.

## Neuropsychological Measures

A subset of 40 older adults (76.4 years; range = 60 to 93; 13 male) completed a battery of psychometric tests as part of more ongoing assessments of structure and cognition in our older adult participant pool. Individual psychometric tests were combined based on functional domains into three composite scores that assessed executive function, memory, and processing speed ability. Table 1 shows the individual test means as well as their grouping into composite scores. To compute composite scores, raw test scores for each individual were converted to *z*-

scores using the group mean for each test, and the *z*-scores for all tests within each composite were summed for each individual. The executive composite combined test scores from the Category Fluency Test (Animals), the Word Fluency Test, the Trail-making Test B, and the Weschler Memory Scale-Revised (WMS-R) Digit Span Test (backward). The memory composite included the WMS Associate Memory Recall Test (hard items), the WMS-R Logical Memory Recall Test, and the Benton Visual Retention Test (Form C, with a delay). The processing speed composite included the Trailmaking Test A, the Crossing Off Test, and Wechsler Adult Intelligence Scale (WAIS) Digit Symbol Test (see Table 1 for test scores). These composite scores were entered into regression analyses that compared the cognitive measures to the strength of functional correlations.

## Amyloid Imaging with PIB

Studies of cognitive aging that screen participants based on behavioral measures (e.g., Mini-Mental State Examination [MMSE]; Folstein et al., 1975) and clinical evaluation (e.g., Clinical Dementia Rating [CDR]; Morris, 1993) risk inclusion of individuals who harbor preclinical AD pathology. As is shown in the results, the present study identifies a robust age-associated disruption in functional correlations. To establish that the present aging effects are due to an age-associated cascade independent of AD pathology, we identified a subset of nine older adults shown to be lacking amyloid plaques as measured using PIB (Klunk et al., 2004). The nine older adults (78.0 years; range = 68 to 86; three male) all participated in a separate imaging session within 2 years following the fMRI session. Radiotracers with a high affinity for amyloid were imaged using [$^{11}$C]PIB on a 961 ECAT PET scanner (Siemens, Erlangen, Germany) according to the procedures described previously (Buckner et al., 2005; Mintun et al., 2006). PIB-PET imaging provides an in vivo measure of human brain amyloid in plaques associated with AD (Klunk et al., 2004). Individuals were considered PIB-negative if their binding potential for four critical regions was below 0.2 (Mintun et al., 2006). For the purposes of the present study, we used PIB-PET imaging to identify a subset of nine older individuals who were free from significant amyloid deposition. Exploration of the distribution of functional correlations in these PIB-negative individuals allowed us to establish that the functional correlation reductions were present independent of undetected, preclinical AD.

## Supplementary Material

Refer to Web version on PubMed Central for supplementary material.

## Acknowledgments

## References

Aizenstein HJ, Clark KA, Butters MA, Cochran J, Stenger VA, Meltzer CC, Reynolds CF, Carter CS. The BOLD hemodynamic response in healthy aging. J Cogn Neurosci 2004;16:786–793. [PubMed: 15200706]

Anand A, Li Y, Wang Y, Wu J, Gao S, Bukhari L, Mathews VP, Kalnin A, Lowe MJ. Activity and connectivity of brain mood regulating circuit in depression: a functional magnetic resonance study. Biol Psychiatry 2005;57:1079–1088. [PubMed: 15866546]

Bäckman L, Ginovart N, Dixon RA, Wahlin TB, Halldin C, Farde L. Age-related cognitive deficits mediated by changes in the striatal dopamine system. Am J Psychiatry 2000;157:635–637. [PubMed: 10739428]

Biswal B, Yetkin FZ, Haughton VM, Hyde JS. Functional connectivity in the motor cortex of resting human brain using echo-planar MRI. Magn Reson Med 1995;34:537–541. [PubMed: 8524021]

Buckner RL. Memory and executive function in aging and AD: multiple factors that cause decline and reserve factors that compensate. Neuron 2004;44:195–208. [PubMed: 15450170]

Buckner RL, Carroll DC. Self-projection and the brain. Trends Cogn Sci 2007;11:49–57. [PubMed: 17188554]

Buckner RL, Snyder AZ, Sanders AL, Raichle ME, Morris JC. Functional brain imaging of young, nondemented, and demented older adults. J Cogn Neurosci 2000;12:24–34. [PubMed: 11506645]

Buckner RL, Head D, Parker J, Fotenos AF, Marcus D, Morris JC, Snyder AZ. A unified approach for morphometric and functional data analysis in young, old, and demented adults using automated atlas-based head size normalization: reliability and validation against manual measurement of total intracranial volume. Neuroimage 2004;23:724–738. [PubMed: 15488422]

Buckner RL, Snyder AZ, Shannon BJ, LaRossa G, Sachs R, Fotenos AF, Sheline YI, Klunk WE, Mathis CA, Morris JC, Mintun MA. Molecular, structural, and functional characterization of Alzheimer's disease: evidence for a relationship between default activity, amyloid, and memory. J Neurosci 2005;25:7709–7717. [PubMed: 16120771]

Cabeza R. Hemispheric asymmetry reduction in older adults: the HAROLD model. Psychol Aging 2002;17:85–100. [PubMed: 11931290]

Cherkassky VL, Kana RK, Keller TA, Just MA. Functional connectivity in a baseline resting-state network in autism. Neuroreport 2006;17:1687–1690. [PubMed: 17047454]

Conturo TE, McKinstry RC, Akbudak E, Robinson BH. Encoding of anisotropic diffusion with tetrahedral gradients: a general mathematical diffusion formalism and experimental results. Magn Reson Med 1996;35:399–412. [PubMed: 8699953]

Corbetta M, Shulman GL. Control of goal-directed and stimulus-driven attention in the brain. Nat Rev Neurosci 2002;3:201–215. [PubMed: 11994752]

De Luca M, Smith SM, De Stefano N, Federico A, Matthews PM. Blood oxygenation level dependent contrast resting state networks are relevant to activity in the neocortical sensorimotor system. Exp Brain Res 2005;167:587–594. [PubMed: 16284751]

D'Esposito M, Deouell LY, Gazzaley A. Alterations in the BOLD fMRI signal with ageing and disease: a challenge for neuroimaging. Nat Rev Neurosci 2003;4:863–872. [PubMed: 14595398]

Folstein MF, Folstein SE, McHugh PR. "Mini-mental state." A practical method for grading the cognitive state of patients for the clinician. J Psychiatr Res 1975;12:189–198. [PubMed: 1202204]

Fox MD, Snyder AZ, Vincent JL, Corbetta M, Van Essen DC, Raichle ME. The human brain is intrinsically organized into dynamic, anticorrelated functional networks. Proc Natl Acad Sci USA 2005;102:9673–9678. [PubMed: 15976020]

Fox MD, Corbetta M, Snyder AZ, Vincent JL, Raichle ME. Spontaneous neuronal activity distinguishes human dorsal and ventral attention systems. Proc Natl Acad Sci USA 2006;103:10046–10051. [PubMed: 16788060]

Fransson P. Spontaneous low-frequency BOLD signal fluctuations: an fMRI investigation of the resting-state default mode of brain function hypothesis. Hum Brain Mapp 2005;26:15–29. [PubMed: 15852468]

Gazzaley A, Cooney JW, Rissman J, D'Esposito M. Top-down suppression deficit underlies working memory impairment in normal aging. Nat Neurosci 2005;8:1298–1300. [PubMed: 16158065]

Geschwind N. Disconnexion syndromes in animals and man. Brain 1965;88:237–294. 585–644. [PubMed: 5318481]

Grady CL, McIntosh AR, Craik FI. Age-related differences in the functional connectivity of the hippocampus during memory encoding. Hippocampus 2003;13:572–586. [PubMed: 12921348]

Greicius MD, Krasnow B, Reiss AL, Menon V. Functional connectivity in the resting brain: a network analysis of the default mode hypothesis. Proc Natl Acad Sci USA 2003;100:253–258. [PubMed: 12506194]

Greicius MD, Srivastava G, Reiss AL, Menon V. Default-mode network activity distinguishes Alzheimer's disease from healthy aging: evidence from functional MRI. Proc Natl Acad Sci USA 2004;101:4637–4642. [PubMed: 15070770]

He BJ, Snyder AZ, Vincent JL, Epstein A, Shulman GL, Corbetta M. Breakdown of functional connectivity in frontoparietal networks underlies behavioral deficits in spatial neglect. Neuron 2007;53:905–918. [PubMed: 17359924]

Head D, Buckner RL, Shimony JS, Williams LE, Akbudak E, Conturo TE, McAvoy M, Morris JC, Snyder AZ. Differential vulnerability of anterior white matter in nondemented aging with minimal acceleration in dementia of the Alzheimer type: evidence from diffusion tensor imaging. Cereb Cortex 2004;14:410–423. [PubMed: 15028645]

Hedden T, Gabrieli JD. Insights into the ageing mind: a view from cognitive neuroscience. Nat Rev Neurosci 2004;5:87–96. [PubMed: 14735112]

Klunk WE, Engler H, Nordberg A, Wang Y, Blomqvist G, Holt DP, Bergstrom M, Savitcheva I, Huang GF, Estrada S, et al. Imaging brain amyloid in Alzheimer's disease with Pittsburgh Compound-B. Ann Neurol 2004;55:306–319. [PubMed: 14991808]

Konishi S, Wheeler ME, Donaldson DI, Buckner RL. Neural correlates of episodic retrieval success. Neuroimage 2000;12:276–286. [PubMed: 10944410]

Liang M, Zhou Y, Jiang T, Liu Z, Tian L, Liu H, Hao Y. Widespread functional disconnectivity in schizophrenia with resting-state functional magnetic resonance imaging. Neuroreport 2006;17:209–213. [PubMed: 16407773]

Lustig C, Buckner RL. Preserved neural correlates of priming in old age and dementia. Neuron 2004;42:865–875. [PubMed: 15182724]

Lustig C, Snyder AZ, Bhakta M, O'Brien KC, McAvoy M, Raichle ME, Morris JC, Buckner RL. Functional deactivations: change with age and dementia of the Alzheimer-type. Proc Natl Acad Sci USA 2003;100:14504–14509. [PubMed: 14608034]

Maccotta L, Zacks JM, Buckner RL. Rapid self-paced event-related functional MRI: feasibility and implications of stimulus-versus response-locked timing. Neuroimage 2001;14:1105–1121. [PubMed: 11697942]

Matsunami K, Hamada I. Effects of stimulation of corpus callosum on precentral neuron activity in the awake monkey. J Neurophysiol 1984;52:676–691. [PubMed: 6491712]

Mazoyer B, Zago L, Mellet E, Bricogne S, Etard O, Houde O, Crivello F, Joliot M, Petit L, Tzourio-Mazoyer N. Cortical networks for working memory and executive functions sustain the conscious resting state in man. Brain Res Bull 2001;54:287–298. [PubMed: 11287133]

Mintun MA, Larossa GN, Sheline YI, Dence CS, Lee SY, Mach RH, Klunk WE, Mathis CA, DeKosky ST, Morris JC. [11C]PIB in a nondemented population: potential antecedent marker of Alzheimer disease. Neurology 2006;67:446–452. [PubMed: 16894106]

Morris JC. The Clinical Dementia Rating (CDR): current version and scoring rules. Neurology 1993;43:2412–2414. [PubMed: 8232972]

Myers RE. Commissural connections between occipital lobes of the monkey. J Comp Neurol 1962;118:1–16. [PubMed: 14477697]

O'Sullivan M, Jones DK, Summers PE, Morris RG, Williams SC, Markus HS. Evidence for cortical "disconnection" as a mechanism of age-related cognitive decline. Neurology 2001;57:632–638. [PubMed: 11524471]

Park DC, Polk TA, Park R, Minear M, Savage A, Smith MR. Aging reduces neural specialization in ventral visual cortex. Proc Natl Acad Sci USA 2004;101:13091–13095. [PubMed: 15322270]

Pfefferbaum A, Sullivan EV, Hedehus M, Lim KO, Adalsteinsson E, Moseley M. Age-related decline in brain white matter anisotropy measured with spatially corrected echo-planar diffusion tensor imaging. Magn Reson Med 2000;44:259–268. [PubMed: 10918325]

Pfefferbaum A, Adalsteinsson E, Sullivan EV. Frontal circuitry degradation marks healthy adult aging: evidence from diffusion tensor imaging. Neuroimage 2005;26:891–899. [PubMed: 15955499]

Raichle ME, MacLeod AM, Snyder AZ, Powers WJ, Gusnard DA, Shulman GL. A default mode of brain function. Proc Natl Acad Sci USA 2001;98:676–682. [PubMed: 11209064]

Raz, N. Aging of the brain and its impact on cognitive performance: integration of structural and functional findings. In: Craik, FIM.; Salthouse, TA., editors. The Handbook of Aging and Cognition. Vol. Second Edition. Mahwah, NJ; Erlbaum: 2000. p. 1-90.

Reuter-Lorenz P. New visions of the aging mind and brain. Trends Cogn Sci 2002;6:394–400. [PubMed: 12200182]

Salat DH, Tuch DS, Greve DN, van der Kouwe AJ, Hevelone ND, Zaleta AK, Rosen BR, Fischl B, Corkin S, Rosas HD, Dale AM. Age-related alterations in white matter microstructure measured by diffusion tensor imaging. Neurobiol Aging 2005;26:1215–1227. [PubMed: 15917106]

Shulman GL, Fiez JA, Corbetta M, Buckner RL, Miezin FM, Raichle ME, Petersen SE. Common blood flow changes across visual tasks: II: decreases in cerebral cortex. J Cogn Neurosci 1997;9:648–663.

Sullivan EV, Pfefferbaum A. Diffusion tensor imaging and aging. Neurosci Biobehav Rev 2006;30:749–761. [PubMed: 16887187]

Talairach, J.; Tournoux, P. Co-Planar Stereotaxic Atlas of the Human Brain. New York: Thieme Medical Publishers, Inc.; 1988.

Tian L, Jiang T, Wang Y, Zang Y, He Y, Liang M, Sui M, Cao Q, Hu S, Peng M, Zhuo Y. Altered resting-state functional connectivity patterns of anterior cingulate cortex in adolescents with attention deficit hyperactivity disorder. Neurosci Lett 2006;400:39–43. [PubMed: 16510242]

Vincent JL, Snyder AZ, Fox MD, Shannon BJ, Andrews JR, Raichle ME, Buckner RL. Coherent spontaneous activity identifies a hippocampal-parietal memory network. J Neurophysiol 2006;96:3517–3531. [PubMed: 16899645]

Vincent JL, Patel GH, Fox MD, Snyder AZ, Baker JT, Van Essen DC, Zempel JM, Snyder LH, Corbetta M, Raichle ME. Intrinsic functional architecture in the anaesthetized monkey brain. Nature 2007;447:83–86. [PubMed: 17476267]

Wu T, Zang Y, Wang L, Long X, Hallet M, Chen Y, Li K, Chan P. Aging influence on functional connectivity of the motor network in the resting state. Neurosci Lett 2007;422:164–168. [PubMed: 17611031]

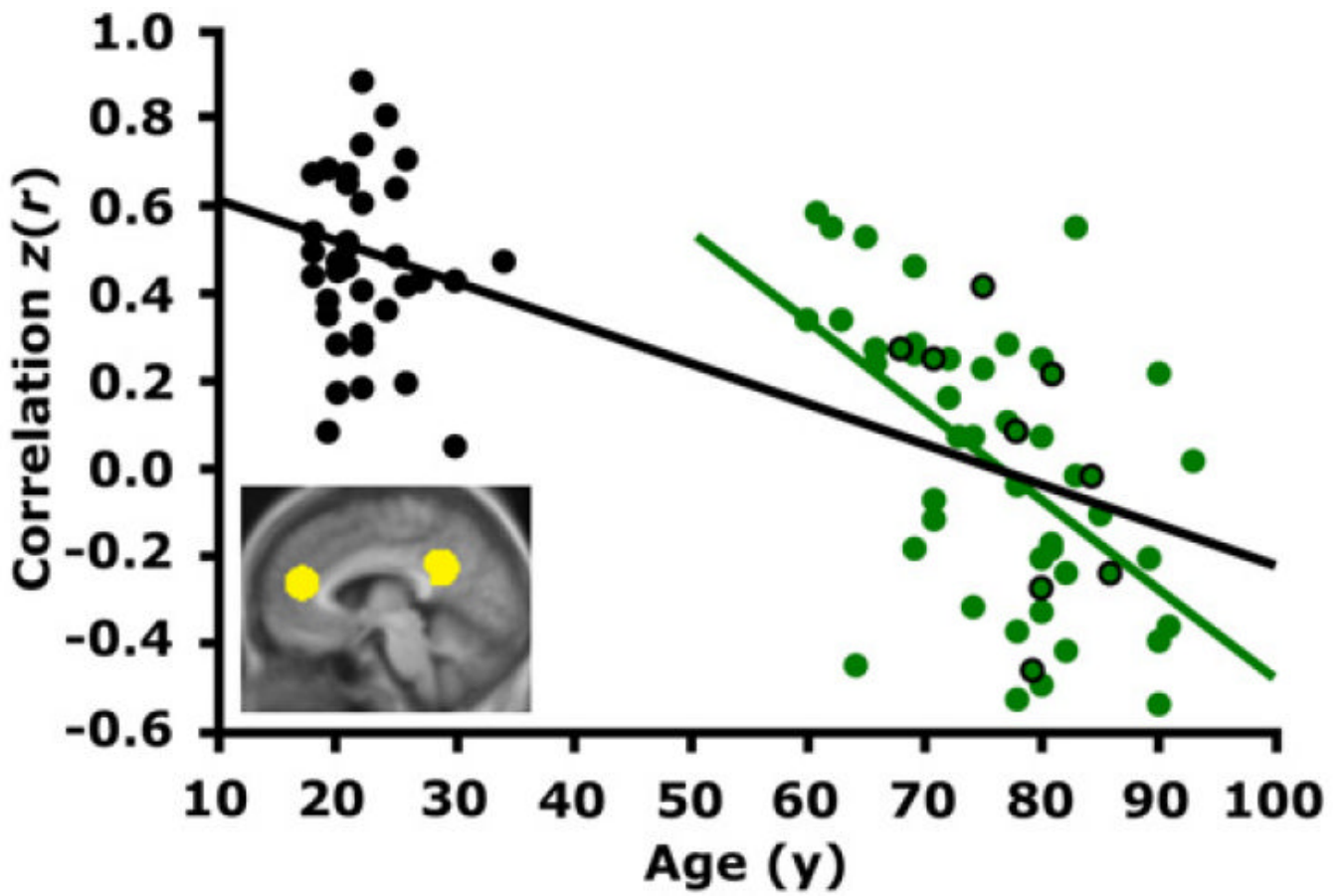Zar, JH. Biostatistical Analysis. Upper Saddle River: Prentice-Hall; 1996.

**Figure 1. Anterior to Posterior Functional Correlations Are Markedly Reduced in Advanced Aging**
The time course within the medial prefrontal cortex (mPFC) was correlated with the time course within the posterior cingulate/retrosplenial cortex (pC/rsp) for each participant. The resulting z-transformed correlation coefficient $z(r)$ for each participant is plotted against age. Data representing young adult participants are colored in black, and those representing older adult participants are colored in green. The black regression line, shown for illustrative purposes only, indicates a strong negative relationship between anterior-posterior functional correlations and age across both groups. The green regression line indicates a negative relationship with age in the older group alone ($r = -0.53$, $p < 0.001$). Green data points outlined in black represent PIB-negative individuals. Importantly, their scattered distribution suggests that the age-dependent decline in anterior-posterior functional correlations exists independently of preclinical AD.
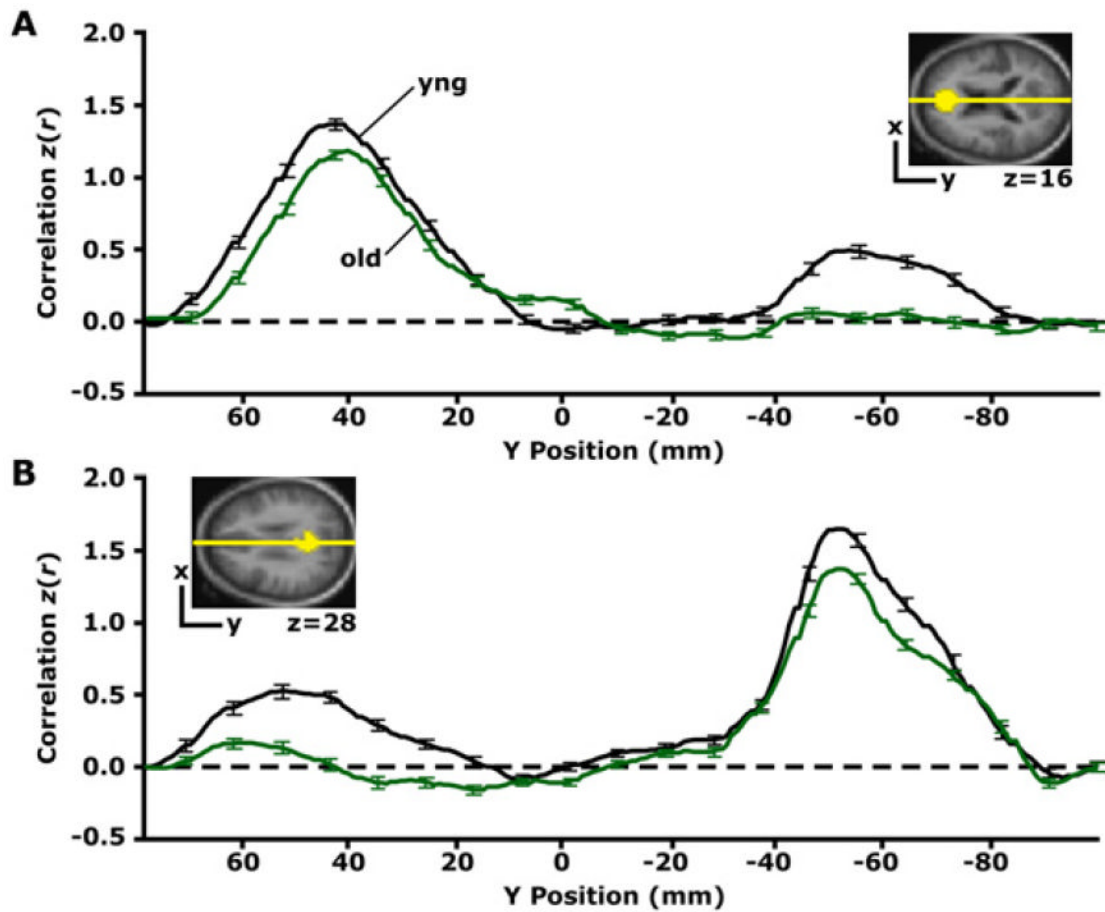
**Figure 2. Reduced Functional Correlations Observed Anatomically**
(A) The time course within the mPFC seed region, shown in yellow for only one transverse slice (z = 16) illustrated in the upper right, was correlated with every voxel in the brain. The graph displays the group-averaged *z*-transformed correlation coeffecient, *z*(*r*), plotted along a line connecting the center of the mPFC seed and the pC/rsp target regions (shown in [B]), for the anterior-posterior axis. This line is graphically represented in yellow on the transverse slice. The first leftward peak in the graph illustrates that the highest *z*(*r*) for both groups is localized to the mPFC seed region. Notice that although the young adult group (black line) exhibits functional correlations with the pC/rsp (indicated by the rightward peak), these correlations are minimally present in the older adult group. (B) A similar analysis was performed for a seed in the pC/rsp, shown for a single transverse slice illustrated in the upper left (z = 28). The yellow line is a graphical representation of a line connecting the center of the seed and the mPFC target (shown in [A]). The group-averaged *z*-transformed correlation coefficients are sampled along the line and plotted against the y position for both groups (black = young; green = old). Error bars = SEM.
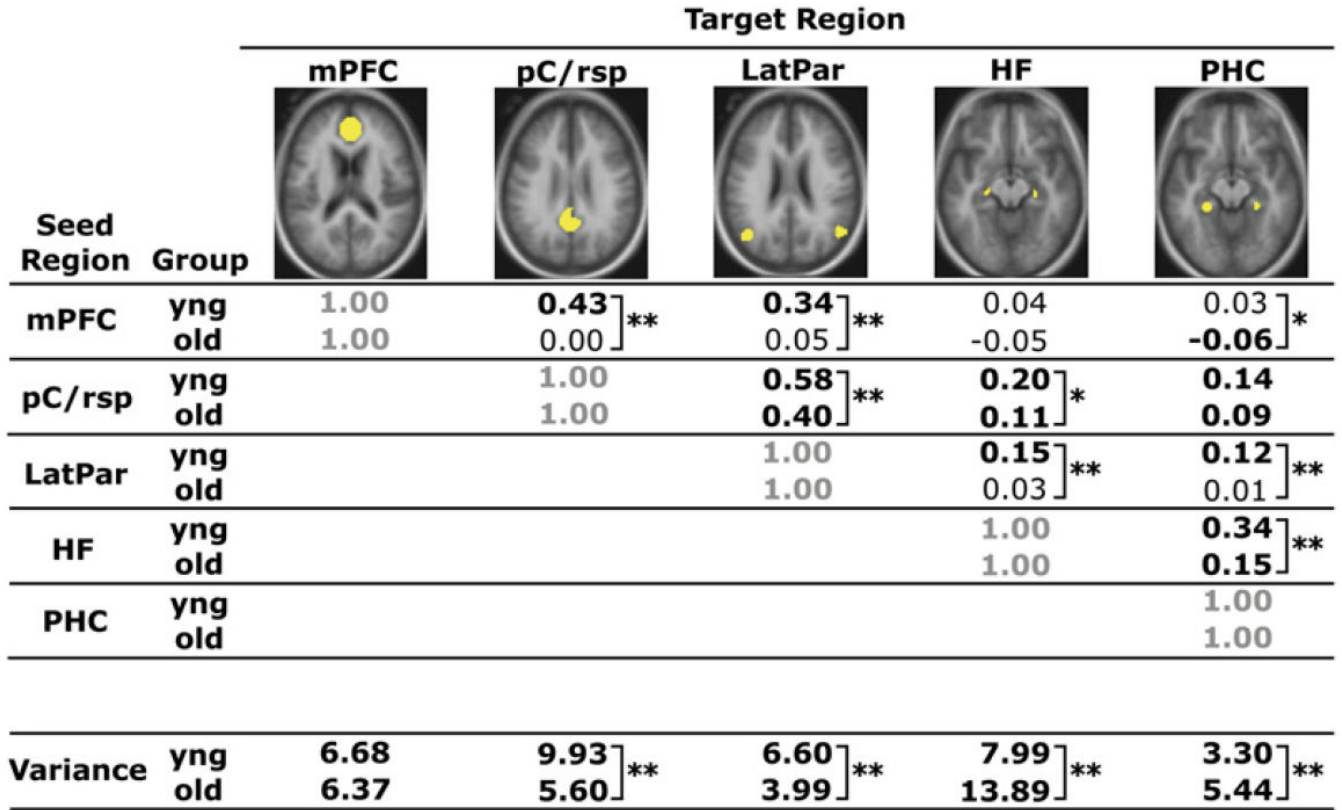
**Target Region**

| Seed Region | Group | mPFC | pC/rsp | LatPar | HF | PHC |
|---|---|---|---|---|---|---|
| mPFC | yng | 1.00 | **0.43** ⎤ ** | **0.34** ⎤ ** | 0.04 | 0.03 ⎤ * |
|  | old | 1.00 | 0.00 ⎦ | 0.05 ⎦ | -0.05 | **-0.06** ⎦ |
| pC/rsp | yng |  | 1.00 | **0.58** ⎤ ** | **0.20** ⎤ * | **0.14** |
|  | old |  | 1.00 | **0.40** ⎦ | **0.11** ⎦ | **0.09** |
| LatPar | yng |  |  | 1.00 | **0.15** ⎤ ** | **0.12** ⎤ ** |
|  | old |  |  | 1.00 | **0.03** ⎦ | **0.01** ⎦ |
| HF | yng |  |  |  | 1.00 | **0.34** ⎤ ** |
|  | old |  |  |  | 1.00 | **0.15** ⎦ |
| PHC | yng |  |  |  |  | 1.00 |
|  | old |  |  |  |  | 1.00 |
| Variance | yng | 6.68 | 9.93 ⎤ ** | 6.60 ⎤ ** | 7.99 ⎤ ** | 3.30 ⎤ ** |
|  | old | 6.37 | 5.60 ⎦ | 3.99 ⎦ | 13.89 ⎦ | 5.44 ⎦ |

**Figure 3. Reduced Functional Correlations Are Observed between Multiple Regions within the Large-Scale Brain System**

Correlation coefficients between a priori seed and target regions that comprise a large-scale brain system (the default network) are quantified for each group, with values significantly different from zero highlighted in bold (mPFC versus PHC: $p < 0.05$; all others: $p < 0.001$). The regions illustrated in yellow include the mPFC, pC/rsp, bilateral lateral parietal cortex (LatPar), bilateral hippocampal formation (HF), and bilateral parahippocampal cortex (PHC). The mean variance computed as the mean of the within-subject variances for each participant's time course within each region is also listed at the bottom of the table. **Group t test significant at a Bonferroni corrected alpha of 0.005. *Group t test significant at an uncorrected alpha of 0.05.
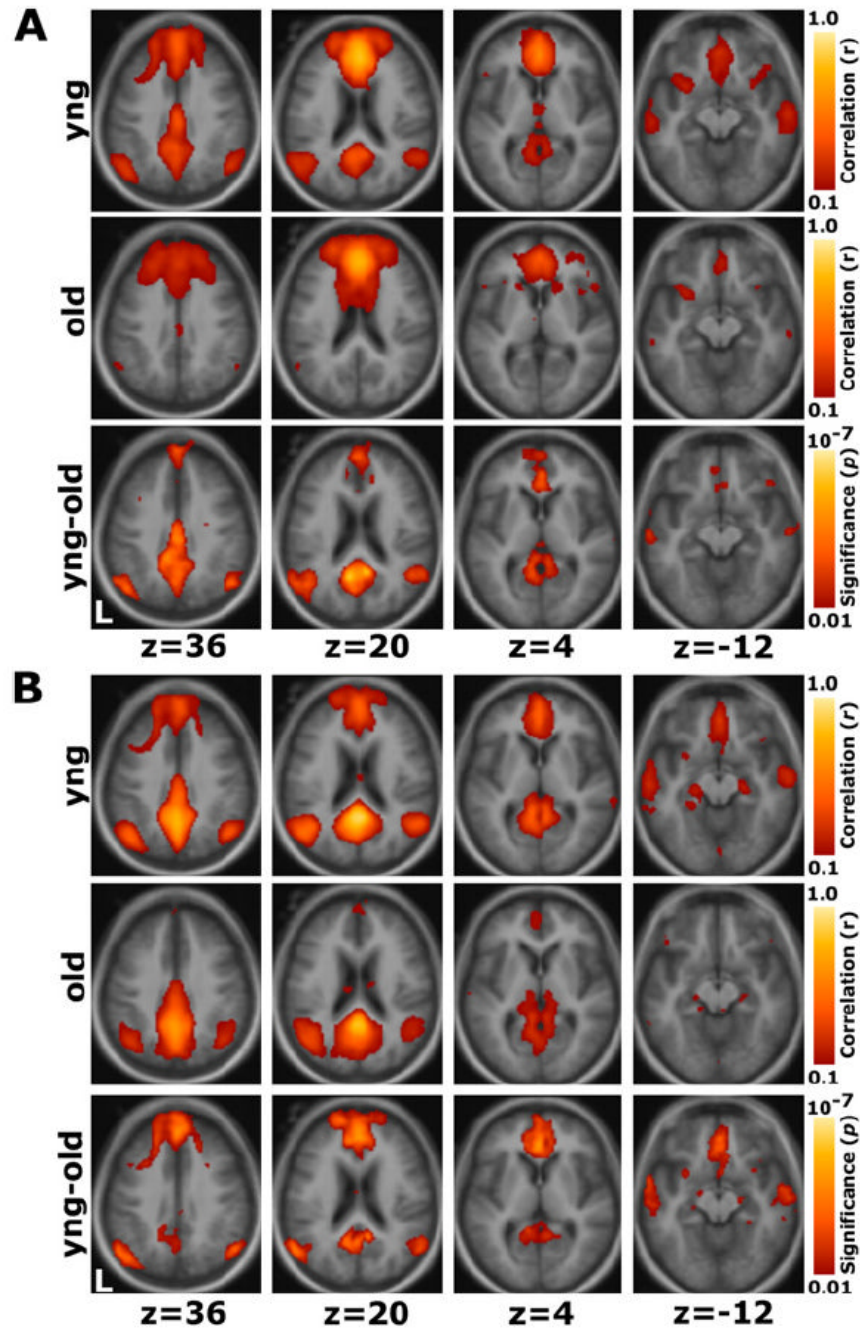
**Figure 4. Whole-Brain Exploratory Analyses Reveal Widespread Correlation Reductions in Aging**
Whole-brain analyses of functional correlations between the seed region and each voxel across the entire brain are graphically overlaid on a combined young and old adult anatomical image. (A) For a seed placed in the mPFC, positive correlations with the mPFC time course exceeding a threshold of $r = 0.1$ are colored in red to yellow and averaged for all young participants (top) and all old participants (middle). A direct comparison between the two groups using the young-old contrast (bottom) highlights voxels at a significance level of $p < 0.01$. The young group shows higher correlations with many regions comprising the network.

(B) The reverse scenario when a seed is placed in the pC/rsp. Functional correlations between the pC/rsp and both the mPFC and the bilateral LatPar, as well as some hint of the HF, decline in old age.

| Seed Region | Group | Target Region | | | | |
|---|---|---|---|---|---|---|
| | | IPS | vIPS | FEF | PrCeS | MT+ |
| IPS | yng | 1.00 | 0.47 ⎤* | 0.11 | 0.21 | 0.23 ⎤** |
| | old | 1.00 | 0.38 ⎦ | 0.11 | 0.20 | 0.06 ⎦ |
| vIPS | yng | | 1.00 | 0.06 ⎤* | 0.22 ⎤* | 0.30 ⎤** |
| | old | | 1.00 | -0.02 ⎦ | 0.08 ⎦ | 0.15 ⎦ |
| FEF | yng | | | 1.00 | 0.17 ⎤* | -0.01 |
| | old | | | 1.00 | 0.28 ⎦ | 0.01 |
| PrCeS | yng | | | | 1.00 | -0.03 |
| | old | | | | 1.00 | 0.03 |
| MT+ | yng | | | | | 1.00 |
| | old | | | | | 1.00 |
| Variance | yng | 4.35 | 2.42 | 2.60 | 3.52 | 2.43 |
| | old | 5.30 | 3.10 | 3.11 | 2.99 | 2.71 |

**Figure 5. Reduced Functional Correlations Are Present in the Dorsal Attention System**
Correlation coefficients between a priori seed and target regions that comprise the dorsal attention system are quantified for each group, with values significantly different from zero highlighted in bold (all: p < 0.05). The regions illustrated in yellow include the intraparietal sulcus (IPS), ventral intraparietal sulcus (vIPS), frontal eye fields (FEF), inferior precentral sulcus (PrCeS), and middle temporal area (MT+). The mean variance, computed as the mean of the within-subject variances for each participant's time course within each region, is also listed at the bottom of the table. **Group t test significant at a Bonferroni corrected alpha of 0.005. *Group t test significant at a Bonferroni corrected alpha of 0.005. *Significant at an uncorrected alpha of 0.05.
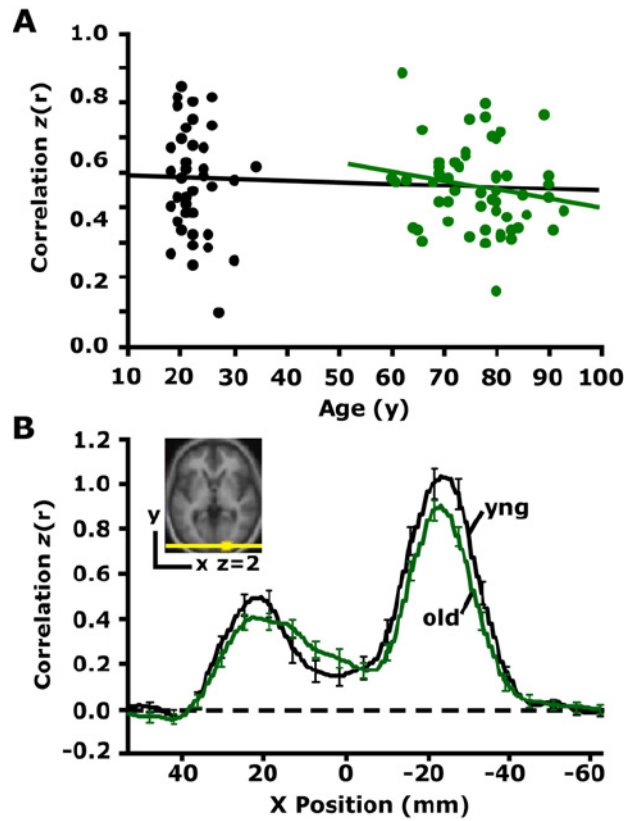
**Figure 6. Functional Correlations between the Left and Right Visual Cortex Are Preserved in Aging**
(A) The time course was extracted from a region within the right visual cortex (see inset in [B]) and correlated with the time course extracted from the left visual cortex for each participant. The resulting correlation coefficients are plotted against age. The black regression line, used here for illustrative purposes only, suggests that interhemispheric functional correlations in visual cortex remain constant with age. The green regression line illustrates the same effect in the older group alone ($r = -0.17$, p = 0.22). (B) Exploratory analyses for a seed in the right visual cortex (see inset) are plotted along a line connecting the center of the right and left visual cortex. For each voxel positioned along the x axis, the mean $z$-transformed correlation of all young adults is shown in black, and the mean $z$-transformed correlation of all old adults is shown in green. The rightward $z$-transformed correlation coefficient peak represents functional correlations at the seed (right visual cortex), and the leftward peak represents functional correlations at the target (left visual cortex). Error bars = SEM.
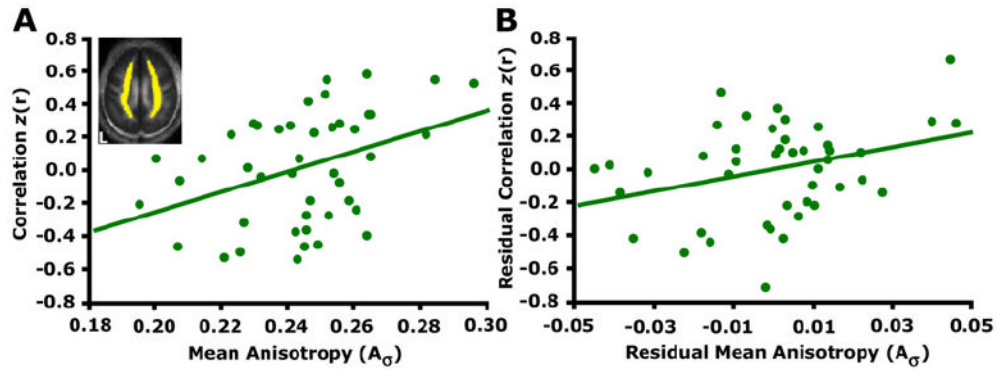
**Figure 7. Functional Correlations Relate to White Matter Integrity in Older Adults**
(A) Mean anisotropy for a white matter region shown in yellow on one transverse slice was extracted for each participant. The correlation coefficients resulting from correlating the mPFC and pC/rsp time course are plotted against the mean anisotropy ($A_\sigma$) ($r = 0.39$, p < 0.05).
(B) A linear regression was performed using the same measures, after controlling for the effect of age on each measure. When doing so, the strength of the relationship between the anterior-posterior functional correlations and white matter integrity remained significant (partial $r = 0.33$, p < 0.05).
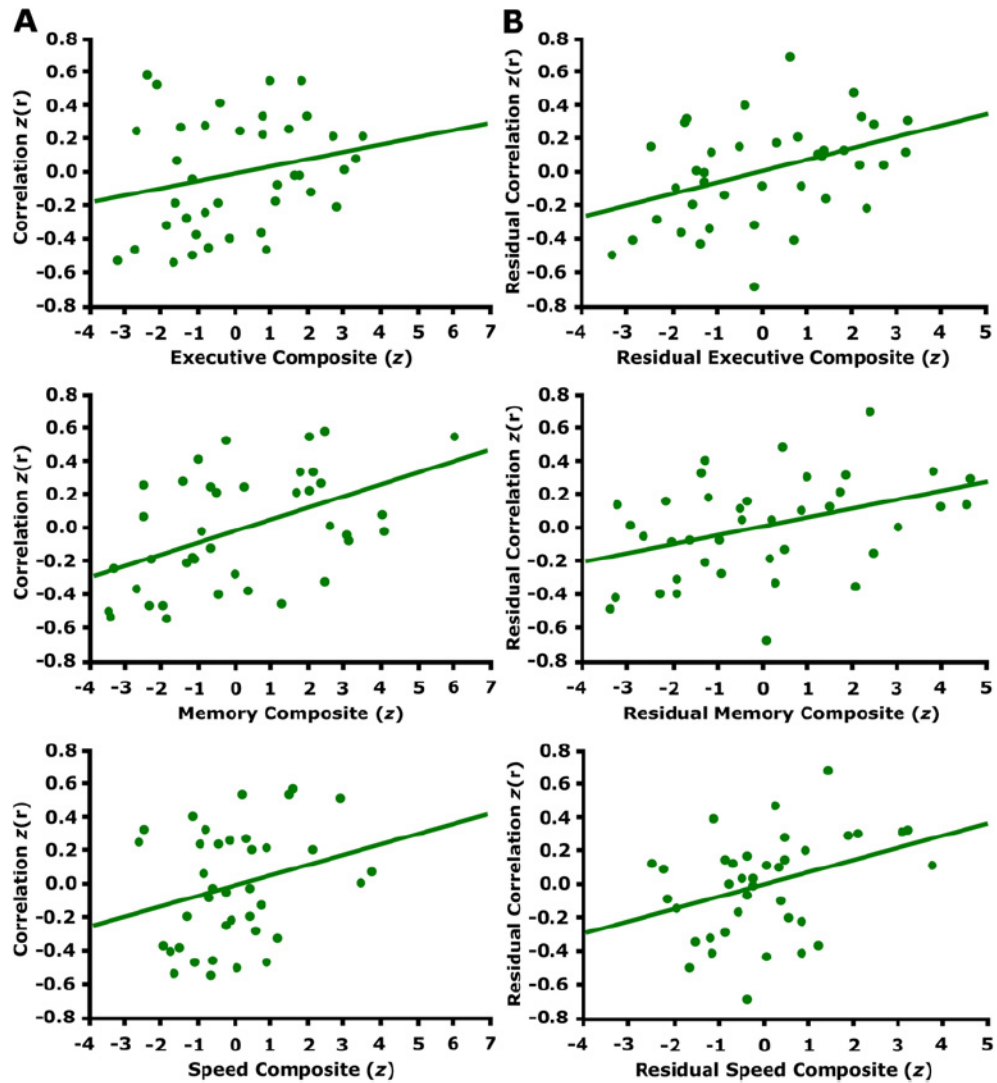
**Figure 8. Functional Correlations Relate to Cognitive Performance in Older Adults**
(A) The *z*-transformed correlation coefficients resulting from correlating the mPFC and pC/rsp time course is plotted against the cognitive test scores (converted to *z*-scores) for three different cognitive components (see text for details). The regression lines between the two measures are plotted on each graph. The memory component significantly associates with anterior-posterior functional correlations (executive: $r = 0.26$, p = 0.11; memory: $r = 0.48$, p < 0.01; speed: $r = 0.24$, p = 0.14).
(B) A linear regression was performed using the same measures as in (A), after controlling for the effect of age on each measure. When doing so, anterior-posterior functional correlations significantly associated with all three cognitive components (executive: partial $r = 0.41$, p < 0.01; memory: partial $r = 0.40$, p < 0.01; speed: $r = 0.35$, p < 0.05).

**Table 1**

Participant Demographics

|  | Young (SD) | Old (SD) |
|---|---|---|
| N | 38 | 55 |
| Mean age (year) | 22.4 (3.6) | 76.5 (8.2) |
| Age range | 18–34 | 60–93 |
| Percent male | 47.3 | 32.7 |
| Education (year) | n/a | 14.1[a] |
| MMSE | n/a | 28.8[b] |
| CDR | n/a | all CDR 0 |
| Executive Composite |  |  |
|   WMS-R Digit Span (backward) | 5.2 (1.2) |  |
|   Trailmaking Test B (s) | 100.0 (40.2) |  |
|   Word Fluency Test | 30.6 (9.0) |  |
|   Category Fluency Test (Animals) | 20.2 (5.1) |  |
| Memory Composite |  |  |
|   WMS-R Logical Memory Recall | 7.8 (4.0) |  |
|   WMS-R Associates Recall - hard | 6.6 (3.4) |  |
|   Benton Visual Retention Test C - delay | 6.1 (1.7) |  |
| Processing Speed Component |  |  |
|   Trailmaking Test A (s) | 36.6 (11.5) |  |
|   Crossing Off Test ((# lines/s) × 100) | 163.7 (31.3) |  |
|   WAIS Digit Symbol Test | 46.2 (9.0) |  |

MMSE = Mini-Mental State Examination (Folstein et al., 1975); CDR = Clinical Dementia Rating where CDR = 0 is nonde-mented (Morris, 1993); WMS-R = Wechsler Memory Scale-Revised; WAIS = Wechsler Adult Intelligence Scale.

[a] Information available from 43 participants.

[b] Information available from 40 participants.